



Contents lists available at ScienceDirect

EBioMedicine

journal homepage: www.ebiomedicine.com
EBioMedicine
 Published by THE LANCET

Endoplasmic reticulum stress is activated in post-ischemic kidneys to promote chronic kidney disease

 Shaoqun Shu ^a, Jiefu Zhu ^{a,b}, Zhiwen Liu ^a, Chengyuan Tang ^a, Juan Cai ^a, Zheng Dong ^{a,b,*}
^a Department of Nephrology, The Second Xiangya Hospital at Central South University, Changsha, Hunan, China

^b Department of Cellular Biology and Anatomy, Medical College of Georgia at Augusta University and Charlie Norwood VA Medical Center, Augusta, GA, USA

ARTICLE INFO

Article history:

Received 6 August 2018

Received in revised form 22 September 2018

Accepted 2 October 2018

Available online xxxxx

Keywords:

ER stress

AKI-CKD transition

Renal ischemia-reperfusion

Fibrosis

Apoptosis

Autophagy

ABSTRACT

Background: Acute kidney injury (AKI) may lead to the development of chronic kidney disease (CKD), i.e. AKI-CKD transition, but the underlying mechanism remains largely unclear. Endoplasmic reticulum (ER) stress is characterized by the accumulation of unfolded or misfolded proteins in ER resulting in a cellular stress response. The role of ER stress in AKI-CKD transition remains unknown.

Methods: In this study, we examined ER stress in the mouse model of AKI-CKD transition after unilateral renal ischemia-reperfusion injury (uIR). To determine the role of ER stress in AKI-CKD transition, we tested the effects of two chemical chaperones: Tauroursodeoxycholic acid (TUDCA) and 4-phenylbutyric acid (4-PBA).

Findings: uIR led to the induction of ER stress in kidneys, as indicated by increased expression of UPR molecules CHOP (C/EBP homologous protein) and BiP (binding immunoglobulin protein; also called GRP78–78 kDa glucose-regulated protein). Given at 3 days after uIR, both TUDCA and 4-PBA blocked ER stress in post-ischemic kidneys. Notably, both chemicals promoted renal recovery and suppressed tubulointerstitial injury as manifested by the reduction of tubular atrophy, renal fibrosis and myofibroblast activation. Inhibition of ER stress further attenuated renal tubular epithelial cell apoptosis, inflammation and autophagy in post-ischemic kidneys.

Interpretation: These findings suggest that ER stress contributes critically to the development of chronic kidney pathologies and CKD following AKI, and inhibition of ER stress may represent a potential therapeutic strategy to impede AKI-CKD transition.

© 2018 Published by Elsevier B.V. This is an open access article under the CC BY-NC-ND license (<http://creativecommons.org/licenses/by-nc-nd/4.0/>).

1. Introduction

Acute kidney injury (AKI) is a common kidney disease that is characterized by a rapid loss of renal function which is related to high morbidity and mortality [1]. Recently, a number of human epidemiological and experimental animal studies have demonstrated that AKI is not just an acute renal syndrome but also contributes critically to the development and progression of chronic kidney disease (CKD). As a matter of fact, AKI and CKD may not be separate but interconnected diseases of the kidney [2–4]. AKI is pathologically featured by injury and death of renal tubular epithelial cells [5–7]. After initial injury, survival renal tubular cells undergo dedifferentiation and proliferation to replace the injured tubular epithelial cells to restore tubular integrity. Under the condition of severe or episodic AKI, the repair can be incomplete or maladaptive, which usually leads to renal interstitial fibrosis and the progression to CKD [4,8]. Under such conditions, tubular epithelial cells undergo a phenotypic change with persistent production and secretion of profibrotic

factors, leading to the development of chronic renal pathologies (e.g. renal interstitial fibrosis) and CKD. Thus, developing the strategies especially targeting specific mechanisms for impeding AKI-CKD transition is urgently needed. The cellular and molecular basis of AKI-CKD transition is very complex and apparently involves multiple mechanisms, such as maladaptive repair in renal tubules, inflammation, cell cycle arrest, mitochondrial damage, autophagy and senescence, to name just a few [4,8–12].

Endoplasmic reticulum (ER) stress is a cellular stress response to the accumulation of unfolded or misfolded proteins in the ER lumen [11–13]. As such, ER stress is also often called the unfolded protein response (UPR). Currently, three major signaling pathways of UPR have been described, including PERK–eIF2 α –ATF4 pathway, IRE1–XBP1 pathway, and ATF6 pathway. In physiological conditions, the ER stress sensor proteins (PERK, IRE1, ATF6) are bound by the ER chaperone BiP (immunoglobulin-heavy-chain binding protein, also known as GRP78) and maintained in an inactive state. Under ER stress, these proteins dissociate from BiP and then activate downstream signaling pathway to suppress protein translation, upregulate molecular chaperones to enhance protein-folding capacity, and/or promote the degradation of unfolded or misfolded proteins through ER-associated protein

* Correspondence author at: Department of Nephrology, The Second Xiangya Hospital at Central South University, Changsha, Hunan, China.

E-mail addresses: zdong@csu.edu.cn, zdong@augusta.edu (Z. Dong).

<https://doi.org/10.1016/j.ebiom.2018.10.006>

2352–3964/© 2018 Published by Elsevier B.V. This is an open access article under the CC BY-NC-ND license (<http://creativecommons.org/licenses/by-nc-nd/4.0/>).

Please cite this article as: Shu S, et al, Endoplasmic reticulum stress is activated in post-ischemic kidneys to promote chronic kidney disease, EBioMedicine (2018), <https://doi.org/10.1016/j.ebiom.2018.10.006>

Research in context

Evidence before this study

Acute kidney injury (AKI) may lead to the development and progress of chronic kidney disease (CKD). ER stress has been implicated in both AKI and CKD, but its involvement in AKI to CKD transition is largely unclear.

Added value of this study

In this study, we demonstrated ER stress during AKI-CKD transition in the mouse model of unilateral renal ischemia-reperfusion. Notably, inhibition of ER stress with two chemical chaperones promoted renal recovery and suppressed tubulointerstitial pathologies including tubular atrophy, renal fibrosis and myofibroblast activation. Inhibition of ER stress further attenuated renal tubular epithelial cell apoptosis, inflammation and autophagy in post-ischemic kidneys.

Implications of all the available evidence

These findings support a role of ER stress in AKI-CKD transition, suggesting a new therapeutic strategy to impede AKI-CKD transition by blocking ER stress.

degradation (ERAD) pathway. Functionally, depending on the severity and duration of ER stress, UPR can be adaptive or trigger cell death [13–15]. Under the condition of prolonged or severe ER stress that overwhelms the capacity of UPR to restore normal ER function, a pro-apoptotic pathway is initiated to eliminate the affected cell [13–15].

ER stress has been implicated in the pathogenesis of both AKI [7,15–17] and CKD [14,18–23]. However, the involvement of ER stress in AKI-CKD transition remains largely unclear. In this study, we demonstrated the persistent ER stress in post-AKI kidneys, which was involved in the development of chronic renal pathologies and CKD. Mechanistically, sustained ER stress induced renal tubular cell death, inflammation and autophagy. Thus, inhibition of ER stress may represent a potential therapeutic strategy to impede AKI-CKD transition.

2. Materials and methods

2.1. Antibodies and reagents

Primary antibodies used in present study were from following sources: anti-p-PERK (3179S), anti-PERK (3192), anti-BiP (3177S), anti-CHOP(2895), anti-GAPDH (5174), anti- α -Smooth Muscle Actin (19245), anti-vimentin(5741), anti-Caspase-12 (2202S) and anti-Cleaved-Caspase-3 (9664) from Cell Signaling Technology; anti-LC3B (NB100–2220) from Novus Biologicals; anti-collagen 1 (AF7001) from Affinity; anti-CHOP (GB11204) and anti-F4/80 (GB11027) from Servicebio. All secondary antibodies for immunoblot analysis were from Thermo Fisher Scientific. 4-PBA (S4125) and TUDCA (S7896) were from Selleck. TUNEL assay kit (12156792910) was from Roche Life Science. Trizol was from CWBIO. PrimeScript™ RT reagent Kit with gDNA Eraser and TB Green™ Premix Ex Taq II was from TaKaRa.

2.2. Animals and surgical protocol

Male C57BL/6 mice were purchased from SJA Laboratory Animal Corporation (Changsha, Hunan, China) and housed in the pathogen-free animal facility of the second Xiangya Hospital under a 12-h light-dark cycle with free access to food and water. Mice of 8–10 weeks

were used for experiments. Unilateral renal ischemia-reperfusion was operated as recently described [24,25]. Briefly, after anesthetization with pentobarbital (50 mg/kg, i.p.), mice were kept on a Homeothermic Blanket Control Unit (Harvard Apparatus Ltd., U.K.) to monitor and maintain body temperature at ~ 36.5 °C. The left renal pedicle was exposed by flank incisions for unilateral clamping to induce ischemia for 30 min. The clamps were then released for reperfusion. Color change of the kidney was observed to visually monitor ischemia and reperfusion. Sham control mice underwent the same operation without renal pedicle clamping. To evaluate renal function, right nephrectomy was performed 24 h before the mice were sacrificed. Briefly, a flank incision was made to expose the right kidney. Right kidney pedicle was then tied with 4–0 silk and cut to remove the kidney. All animal experiments were conducted in accordance with a protocol approved by the Institutional Animal Care and Use Committee of the Second Xiangya Hospital of Central South University.

2.3. 4-PBA and TUDCA treatment

4-PBA and TUDCA were dissolved in saline and then administrated once daily by intraperitoneal injection from day 3 after ischemic surgery till the day before sacrificing with a dosage of 20 mg/kg/day for 4-PBA and 250 mg/kg/day for TUDCA. Normal saline was injected as vehicle control.

2.4. Assessment of renal function

Right nephrectomy was performed 24 h before the mice were sacrificed for renal function measurement. Serum creatinine was measured by using a commercial kit (DICT-500) from BioAssay Systems as previously described [41]. In brief, blood samples were collected for coagulation and centrifugation at room temperature to collect serum. Serum samples were added to a pre-warmed (37 °C) reaction mixture and the absorbance at 510 nm was monitored kinetically at 0 and 5 min of reaction. Creatinine levels (mg/dl) were then calculated based on standard curves.

2.5. Histological staining

2.5.1. Hematoxylin-eosin staining

Renal tissues were fixed with 4% paraformaldehyde and then embedded in paraffin. Four-micrometer of renal sections were prepared. Hematoxylin-eosin staining was performed to evaluate renal injury following the protocol provided by the manufacturer [51]. Renal tubular atrophy was characterized as tubule dilation with necrotic debris within the lumen and marked expansion of the interstitial space. Quantification of renal tubular atrophy was performed in a blinded manner and scored by the percentage of atrophied tubules: 0, no damage; 1, <25%; 2, 25–50%; 3, 50–75%; 4, >75%.

2.5.2. Periodic acid-schiff staining

Renal tissues were fixed and processed as above. PAS staining was performed using a kit from Servicebio (Wuhan, China) according to a standard procedure staining glycogen-containing components in red-purple.

2.5.3. Masson trichrome staining

Masson trichrome staining was performed to evaluate collagen fibrils in renal tissues by using the reagents from Servicebio. For quantification, 10 to 20 positive collage-stained fields (100 magnification) were randomly selected from each section and analyzed by Image-Pro Plus 6.0. A ratio of blue stained area to the area of entire field (glomeruli, tubule lumina, and blood vessels, if any, excluded) was assessed and expressed as percentage of fibrotic area.

2.6. Immunohistochemical staining of BiP, CHOP and macrophages

Paraffin-embedded kidney sections were deparaffinized and incubated with 0.1 M sodium citrate, PH 6.0 at 65 °C for antigen retrieval. Then the slides were sequentially exposed to 3% H₂O₂ to block endogenous peroxidase activity, a buffer containing 5% BSA and 0.1% Triton X-100 to reduce non-specific binding, a specific primary antibody at 4 °C overnight, and HRP-conjugated secondary antibody for 1 h at room temperature. Signals of the antigen-antibody complexes were detected with a DAB kit following the protocol of the manufacturer. Finally, the slides were counterstained in hematoxylin. For quantification, 10–20 fields were randomly selected from each tissue section and the percentage of positive staining tubules or numbers of positive staining cells per mm² were evaluated.

2.7. Immunohistochemical staining of LC3B

A modified immunohistochemical staining protocol was performed as previously described [37]. Briefly, kidney sections were deparaffinized and after rehydration, antigen retrieval was performed by incubation with 1 mM EDTA (pH 8.0) at 95–100 °C for 20 min. The tissue sections were then incubated sequentially with H₂O₂ to block endogenous peroxidase activity, with a blocking buffer (2% bovine serum albumin, 2% normal donkey serum, 0.2% milk, and 0.8% Triton X-100) to reduce non-specific binding, anti-LC3 antibodies at 4 °C overnight. Negative controls were done by replacing the primary antibody with antibody diluent. First, incubating the slides with avidin–biotin blocking reagent (Vector Laboratories, SP-2001), then exposed to biotinylated goat anti-rabbit/mouse secondary antibody (CWBIO) for 10 min at room temperature. After amplifying the signal with Tyramide Signal Amplification Biotin System (Perkin Elmer, NEL700A001KT), the slides were incubated with a VECTASTAIN® ABC kit (Vector Laboratories, PK-6100). Signals of the antigen-antibody complexes were detected with a DAB kit following the protocol of the manufacturer. Finally, the slides were counterstained in hematoxylin. For quantification, 10 representative fields were selected from each tissue section and the amount of LC3B positive dots per mm² was evaluated.

2.8. TUNEL staining

TUNEL staining was performed to identify apoptotic cells in renal tissues using the reagent (12156792910) from Roche Life Science as described previously [27]. Briefly, tissue sections were deparaffinized and pretreated with 0.1 M sodium citrate, PH 6.0 at 65 °C for 30 min and then incubated with a TUNEL reaction mixture for 1 h at 37 °C in a humidified, dark chamber. Positive staining with nuclear DNA fragmentation was detected by fluorescence microscopy. For quantification, 10 representative fields were selected from each tissue section and the amount of TUNEL positive cells per mm² was evaluated.

2.9. Immunoblot analysis

Renal cortical and outer medulla tissues were lysed using 2% SDS buffer with 1% protease inhibitor cocktail (Sigma-Aldrich, P8340). Protein concentration was determined using a Pierce BCA protein assay kit (23225) from Thermo Scientific. Equal amounts of proteins were separated by SDS-polyacrylamide gel and then transferred onto polyvinylidene difluoride membranes. The membranes were blocked with 5% fat-free milk or 5% bovine serum albumin and subsequently incubated with primary antibodies and secondary antibodies. Antigen-antibody complexes on the membranes were detected with an enhanced chemiluminescence kit from Thermo Scientific.

2.10. Quantitative real-time PCR

Total RNA from kidney tissues was extracted with Trizol reagents from CWBIO (China) according to the manufacturer's protocol. cDNA was synthesized using Taqman RT reagents (TaKaRa). Quantitative real-time PCR was performed in triplicate by using the TB Green™ Premix Ex Taq II reagent (TaKaRa) on LightCycler96 Real-Time PCR System. The mRNA levels of MCP-1, TNF- α and IL-6 were normalized by house keeping gene actin-beta (ACTB). The primers set used were listed in Table 1.

2.11. Statistics

All qualitative data are representatives of at least 3 independent experiments which are expressed as means \pm SEM. GraphPad Prism 5 software was used for statistical analyses. Two-tailed unpaired or paired Student *t*-test was used to analyze differences between two groups. *P* < 0.05 was considered significantly different.

3. Results

3.1. Acute ischemic injury leads to chronic kidney problems

To examine the chronic effects of AKI, we performed unilateral renal ischemia-reperfusion (uIR) in mice, a relatively stable model of AKI-CKD transition with minimal animal loss [24]. Briefly, the left kidney of C57BL/6 mice (male, 8–10 week old) was subjected to 30-min ischemia or sham operation followed by reperfusion for 2, 7 or 14 days, while the contralateral kidney was kept untouched. We firstly analyzed the ratio of kidney to body weight. As depicted in Fig. 1A, the ratio of ischemic kidney/body weight increased following acute injury (2 days after ischemia) and then decreased. At day 14, the ratio of the ischemic kidney/body weight was significantly lower than sham-operated kidney. On the contrary, the ratio of contralateral kidney/body weight increased continually during the observation period (Fig. 1B). We then determined the function of the post-ischemic kidney by measuring serum creatinine. To this end, the contralateral kidney was removed at 24 h before collecting blood samples so that the function of the post-ischemic kidney can be evaluated [25]. As shown in Fig. 1C, serum creatinine was significantly higher at 2, 7 and 14 days after uIR as compared to sham-operated control, indicating continuous dysfunction of the ischemically injured kidney. Histological analysis by hematoxylin-eosin staining revealed marked renal tubular damage at 2 days after uIR as indicated by widespread proximal tubular necrosis, cast formation and tubule dilation. At 7 and 14 days, there were tubular dropout, disarrangement of the remaining renal tubule, tubular atrophy characterized by tubular dilation with necrotic debris within the lumen, and marked expansion of the interstitium. At 14 days, some glomeruli appeared contracted (Fig. 1D). Quantification analysis verified a continuous increase of tubular atrophy after initial uIR (Fig. 1E). Periodic Acid-Schiff (PAS) staining was also performed to verify the results of hematoxylin-eosin staining. As shown in Supplementary Fig. 1A, at uIR 2d group, there are mass brush border loss, cast formation and tubular necrosis. At uIR 7d and uIR 14d group, the most prominent

Table 1
Primer sequences used for qRT-PCR.

Gene	Primer sequences	
MCP-1	Forward	5'-TAAAAACCTGGATCGGAACAAA-3'
	Reverse	5'-GCATTAGCTTCAGATTTACGGGT-3'
TNF- α	Forward	5'-GCGACGTGGAACTGGCAGAAG-3'
	Reverse	5'-GCCACAAGCAGGAATGAGAAGAGG-3'
IL-6	Forward	5'-ACTTCCATCCAGTTGCCTTCTTGG-3'
	Reverse	5'-TTAAGCCTCCGACTTGTGAAGTGG-3'
ACTB	Forward	5'-GCTGACAGGATGCAGAAGGA-3'
	Reverse	5'-GTGGACAGTGAGCCAGGAT-3'

morphological change is tubular atrophy. Meanwhile, At uIR 14d group, there are glomerular and tubule basement membrane thickening and fibrotic interstitium expansion. Renal interstitial fibrosis appeared at 7 and 14 days after uIR, as indicated by increased expression of extracellular matrix component marker (collagen 1) and myofibroblast activation marker (α -SMA/ α -smooth muscle actin and vimentin) (Fig. 1F and G). Masson trichrome staining further verified renal interstitial fibrosis in post-IR kidneys (Fig. 1H and I). Masson trichrome staining (in blue) of fibrosis was mostly located in the cortico-medullary boundary junction which is susceptible to renal IRI. Collectively, these findings indicate that acute injury by IRI can induce chronic renal pathologies and functional deterioration.

3.2. ER stress is induced and sustained in renal proximal tubules in post-ischemic kidneys

We evaluated the levels of ER stress in kidney tissues by examining the expression of two UPR molecules, BiP and CHOP. Immunohistochemical staining showed that, in sham-operated kidney tissues, BiP was mainly expressed in the inner medulla, especially in collecting tubules, and almost absent in the cortex (Fig. 2A). In post-ischemic kidneys, high levels of BiP was observed in the cytoplasm of renal tubular cells. Quantitatively, BiP positive proximal tubules increased from 7.3% in sham control to 19.9% at day 2, 21.3% at day 7, and 17.6% at day 14 after uIR (Fig. 2B). Immunoblot analysis further confirmed the sustained increase in BiP expression after uIR (Fig. 2C). PERK phosphorylation was also detected in post-IR kidneys. The ratio of p-PERK/PERK was significantly increased in uIR groups as compared to sham group (Fig. 2C). Similarly, CHOP expression in renal cortex was also continually increased from day 2 to day 14 after uIR (Fig. 2C–F). Notably, the increase of CHOP mainly occurred in the cytoplasm at day 2 after uIR, and, at day 7, accumulation of CHOP in the nucleus was also observed (Fig. 2E). At day 14, a remarkable increase of CHOP occurred in both cytoplasm and nucleus. Taken together, these findings suggest that ER stress is induced and sustained in renal tubule cells in post-ischemic kidneys.

3.3. Inhibition of ER stress after IRI impedes the development of chronic kidney pathologies

4-PBA and TUDCA are chemical chaperons that attenuate ER stress [18,26]. To determine the role of ER stress in AKI-CKD transition, we evaluated the effects of 4-PBA and TUDCA on the development of chronic renal problems in post-uIR kidneys. 4-PBA and TUDCA were given at day 3 after uIR to avoid their interference on initial acute injury. We initially verified their function as ER stress inhibitors by determining the expression of p-PERK, BiP and CHOP. Immunohistochemical staining showed that 4-PBA and TUDCA significantly reduced the expression of BiP in proximal tubules (Fig. 3A and B). Consistently, immunoblot analysis detected their inhibitory effect on p-PERK, BiP and CHOP induction in post-IRI kidneys (Fig. 3C and D). The inhibitory effects of 4-PBA and TUDCA on CHOP induction were also shown by immunostaining of day 7 and 14 post-IRI kidneys (Fig. 3E and F). Thus, these two chemical chaperons could efficiently suppress ER stress in post-IRI kidneys.

We then determined the effect of 4-PBA and TUDCA on AKI-CKD transition in post-IRI kidneys. We first evaluated their effects on the ratio of kidney weight/body weight. 4-PBA prevented the decrease in ischemic kidney weight at day 7 after uIR, but neither 4-PBA nor TUDCA could prevent kidney weight loss at day 14 (Fig. 4A). Nonetheless, these two chemicals prevented the compensatory size/weight increase of the contralateral kidney at day 14 after uIR (Fig. 4B). Functionally, in comparison to vehicle-treated mice, 4-PBA- and TUDCA-treated mice had significant lower levels of serum creatinine when the contralateral kidney was removed, indicating better function of the post-IRI kidney (Fig. 4C). The treated mice also had less tubular atrophy (Fig. 4D, E and Supplementary Fig. 1B). Besides, The glomerular and tubule basement membrane thickening and fibrotic interstitium

expansion were also reduced after treatment with 4-PBA and TUDCA compared to NS treatment at uIR 14d (Supplementary Fig. 1B). Immunoblot analysis showed that 4-PBA- and TUDCA given after uIR suppressed the expression of collagen I, α -SMA and vimentin at day 7 and day 14 (Fig. 4F and G). Masson trichrome staining further confirmed the anti-fibrotic effect of these two ER stress inhibitors (Fig. 4H and I). Collectively, these results suggest that pharmacological inhibition of ER stress after AKI can attenuate the development or progression of CKD.

3.4. Inhibition of ER stress after AKI alleviates tubular apoptosis and interstitial inflammation

Both renal cell death and inflammation have been suggested to contribute to the development of renal interstitial fibrosis [27]. Therefore, we determined whether pharmacological inhibition of ER stress could reduce renal tubular cell death and interstitial inflammation. Tubular cell apoptosis was evaluated by TUNEL (terminal deoxynucleotidyl transferase-mediated dUTP nick end labeling) staining. As shown in Fig. 5A, TUNEL-positive cells was rarely observed in the kidney tissues of sham-control mice with or without 4-PBA treatment, but appeared in post-IRI operated mice kidneys. Quantification analysis showed that treatment with 4-PBA and TUDCA after uIR significantly reduced the number of TUNEL-positive renal tubular cells at both day 7 and day 14 post-IRI (Fig. 5B). In addition, immunoblotting analysis showed that treatment with these two chemicals dramatically reduced the activation of caspase-12 and caspase-3 in kidney tissues (Fig. 5C and D). Together, these findings indicate that inhibition of ER stress after AKI reduces renal tubular cell death.

We further determined the effects of 4-PBA and TUDCA given after AKI on inflammation. Immunostaining analysis of macrophages with the specific F4/80 antibody showed the occurrence of macrophage infiltration into the post-IRI kidney at both day 7 and day 14. Quantification and statistical analysis showed that treatment with 4-PBA and TUDCA after uIR significantly reduced the number of macrophages infiltrating into kidney (Fig. 6A and B). Quantitative reverse-transcriptase polymerase chain reaction (qRT-PCR) analysis of the expression of proinflammatory cytokines, including monocyte chemoattractant protein-1 (MCP-1), Interleukin 6 (IL-6) and tumor necrosis factor α (TNF- α), revealed an increase of these cytokines in kidney tissues of mice at day 7 and 14 after uIR (Fig. 6C, D and E). 4-PBA failed in reducing the expression of these cytokines in kidney tissues of mice at day 7 after uIR, but it appeared to reduce the expression of MCP-1 and IL-6 in kidney tissues at day 14 after uIR. On the other hand, TUDCA significantly reduced the expression of MCP-1 and TNF- α in the injured kidney at day 14 after uIR (Fig. 6C, D and E). Together, these results indicate that inhibition of ER stress after AKI suppresses renal interstitial inflammation.

3.5. Inhibition of ER stress after AKI reduces renal tubular cell autophagy

ER stress may trigger autophagy [28–31]. Moreover, renal tubular autophagy may contribute critically to the development of chronic renal pathologies including interstitial fibrosis [27]. Therefore, we proposed that the induction of renal tubular cell ER stress after uIR may activate autophagy, contributing to renal fibrosis. To this end, we examined the effects of 4-PBA and TUDCA on renal autophagy in post-IRI kidneys. Autophagy was detected by immunohistochemical staining of LC3 to reveal autophagosomes and immunoblot analysis of LC3-II, two commonly used methods for analysis of *in vivo* autophagy. Immunohistochemical staining of LC3 showed some granular, punctate staining in cytoplasm in day 7 and day 14 post-IRI kidneys, indicating the formation of autophagosomes. Treatment with 4-PBA and TUDCA alleviated LC3 punctate staining in both intensity and numbers (Fig. 7A and B). Immunoblot analysis of LC3 further showed LC3B-II accumulation in post-IRI kidneys (Fig. 7C: lanes 3, 5 vs lanes 1), which was diminished by 4-PBA and TUDCA (Fig. 7C: lane 3 vs 4; lane 5 vs 6, 7).

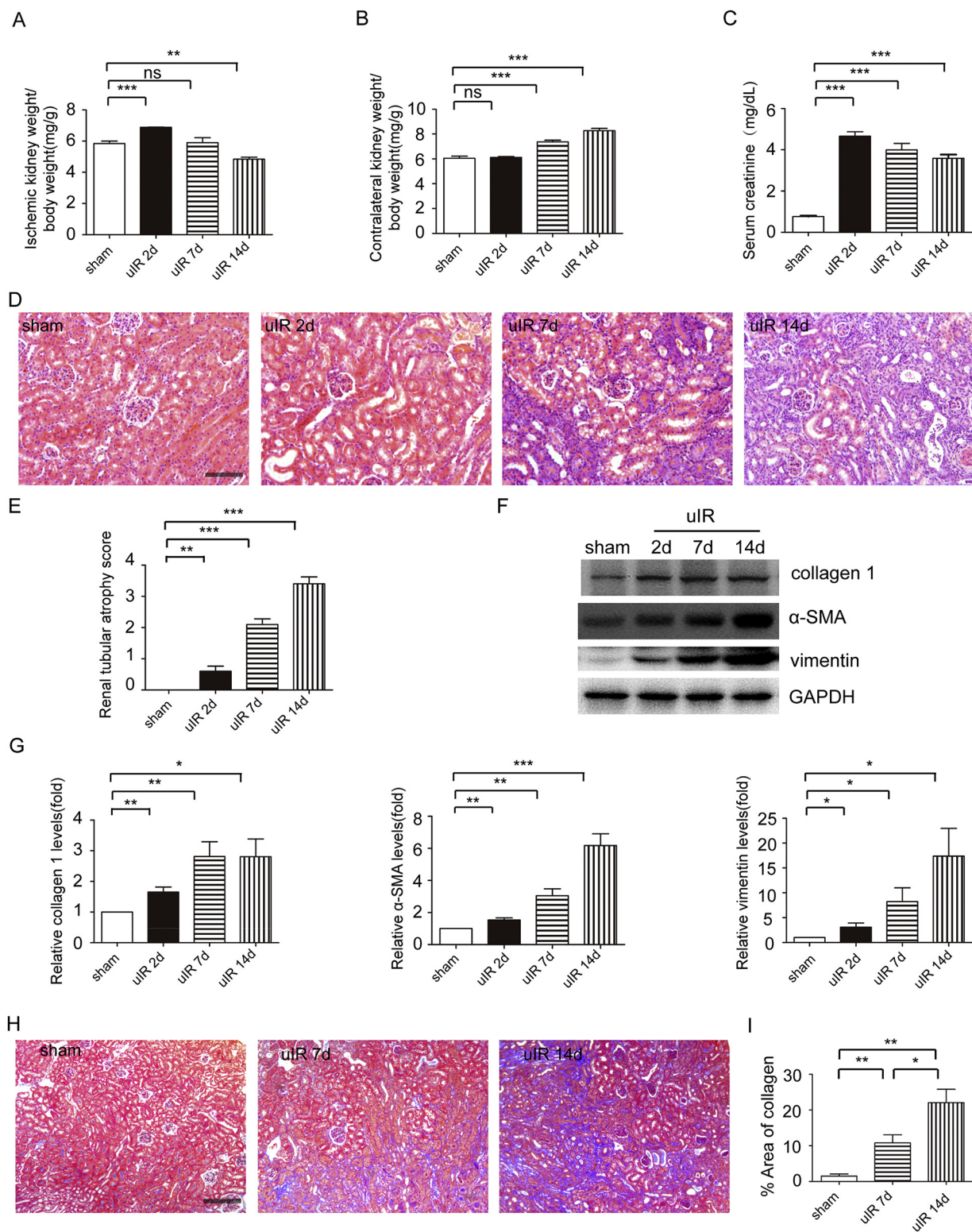


Fig. 1. Unilateral renal ischemia-reperfusion induces chronic kidney problems. C57BL/6 mice (male, 8–10 week old) were subjected to sham operation or 30 min of unilateral ischemia of left kidney followed by reperfusion. For biochemical and histological analyses, kidney tissues were collected at 2, 7 or 14 days after renal ischemia. To determine the function of post-ischemic left kidney, right nephrectomy was performed one day before animal sacrifice and blood samples were then collected at animal sacrifice to measure serum creatinine. (A) Post-ischemic kidney weight/body weight (mg/g). (B) Contralateral kidney weight/body weight (mg/g). (C) Serum creatinine (mg/dL). (D) Representative histology images of hematoxylin-eosin staining. Bar = 200 μ m. (E) Pathological score of tubular atrophy. (F) Representative immunoblots of collagen 1, α -SMA, vimentin, and GAPDH. GAPDH was used as a loading control. (G) Quantitative analysis of immunoblot of collagen 1, α -SMA, and vimentin. For Densitometric analysis, the protein level of sham group was arbitrarily set as 1, and the signals of other conditions were normalized with the sham control group to indicate their protein fold changes. (H) Representative images of Masson trichrome staining. Bar = 200 μ m. (I) Quantitative analysis of Masson trichrome staining. Data are expressed as mean \pm SEM. n = 4. *p < 0.05; **p < 0.01; ***p < 0.001; ns, not significant.

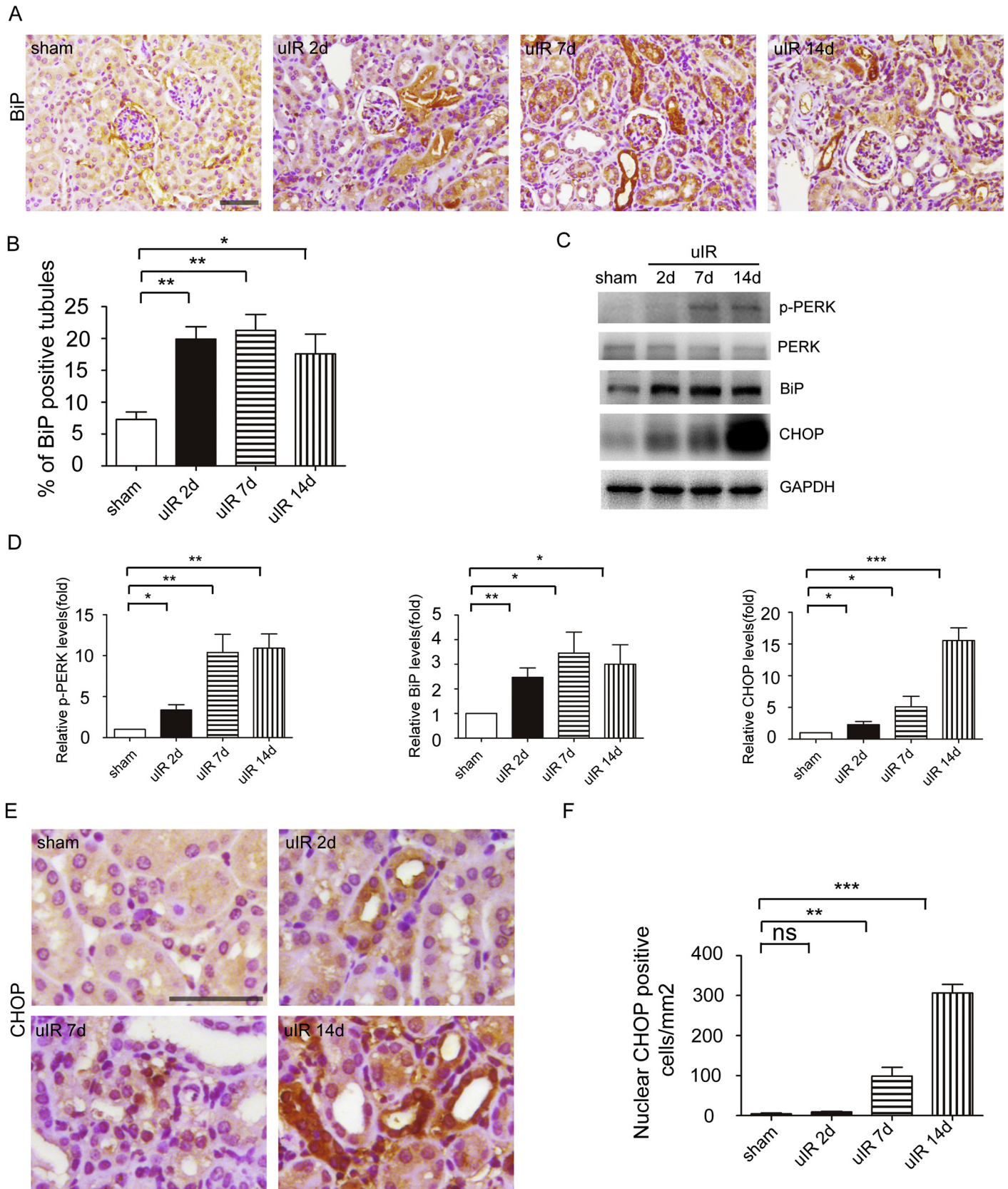


Fig. 2. ER stress is induced and sustained in renal tubules in post-IRI kidney. Mice were subjected to uIR without contralateral nephrectomy or sham-operation as described in Fig. 1. (A) Representative images of immunohistochemical staining of BiP. Bar = 200 μ m. (B) Quantitative analysis of BiP staining. (C) Representative immunoblots of p-PERK, PERK, BiP, CHOP, and GAPDH. GAPDH was used as a loading control. (D) Quantitative analysis of immunoblots of p-PERK, BiP and CHOP. For Densitometric analysis, the protein level of sham group was arbitrarily set as 1, and the signals of other conditions were normalized with the sham control group to indicate their protein fold changes. (E) Representative images of immunohistochemical staining of CHOP. Arrows were used to indicate a few positive activated CHOP proteins. Bar = 200 μ m. (F) Quantitative analysis of CHOP staining. Data are expressed as mean \pm SEM. n = 4 mice. *p < 0.05; **p < 0.01; ***p < 0.001; ns, not significant.

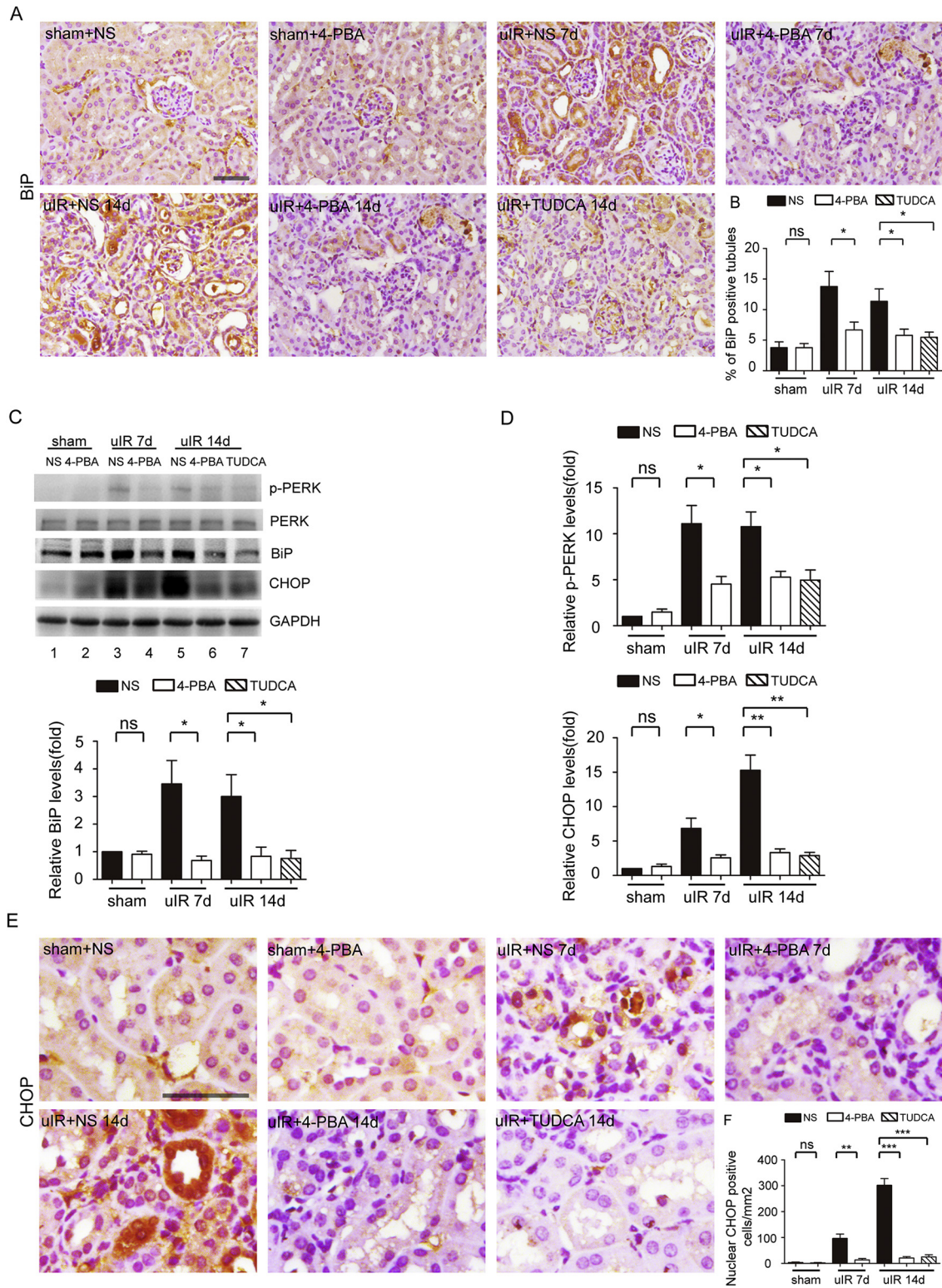


Fig. 3. 4-PBA and TUDCA suppress post-IRI ER stress in kidney tubules. C57Bl/6 mice (male, 8–10 week old) were subjected to 30 min of unilateral ischemia of left kidney followed by reperfusion for 7 or 14 days. 4-PBA at 20 mg/kg/day, TUDCA at 250 mg/kg/day, or normal saline (NS) was given from day 3 after uIR. Then kidney tissues were collected for biochemical and histological analyses. (A) Representative images of immunohistochemical staining of BiP. Bar = 200 μ m. (B) Quantitative analysis of BiP staining. (C) Representative immunoblots of p-PERK, PERK, BiP, CHOP, and GAPDH. GAPDH was used as a loading control. (D) Quantitative analysis of immunoblot signals of p-PERK, BiP and CHOP. For densitometric analysis, the protein level of sham group was arbitrarily set as 1, and the signals of other conditions were normalized with the sham control group to indicate their protein fold changes. (E) Representative images of immunohistochemical staining of CHOP. Arrows point to positive CHOP staining. Bar = 200 μ m. (F) Quantitative analysis of CHOP staining. Data are expressed as mean \pm SEM. n = 4. *p < 0.05; **p < 0.01; ***p < 0.001; ns, not significant.

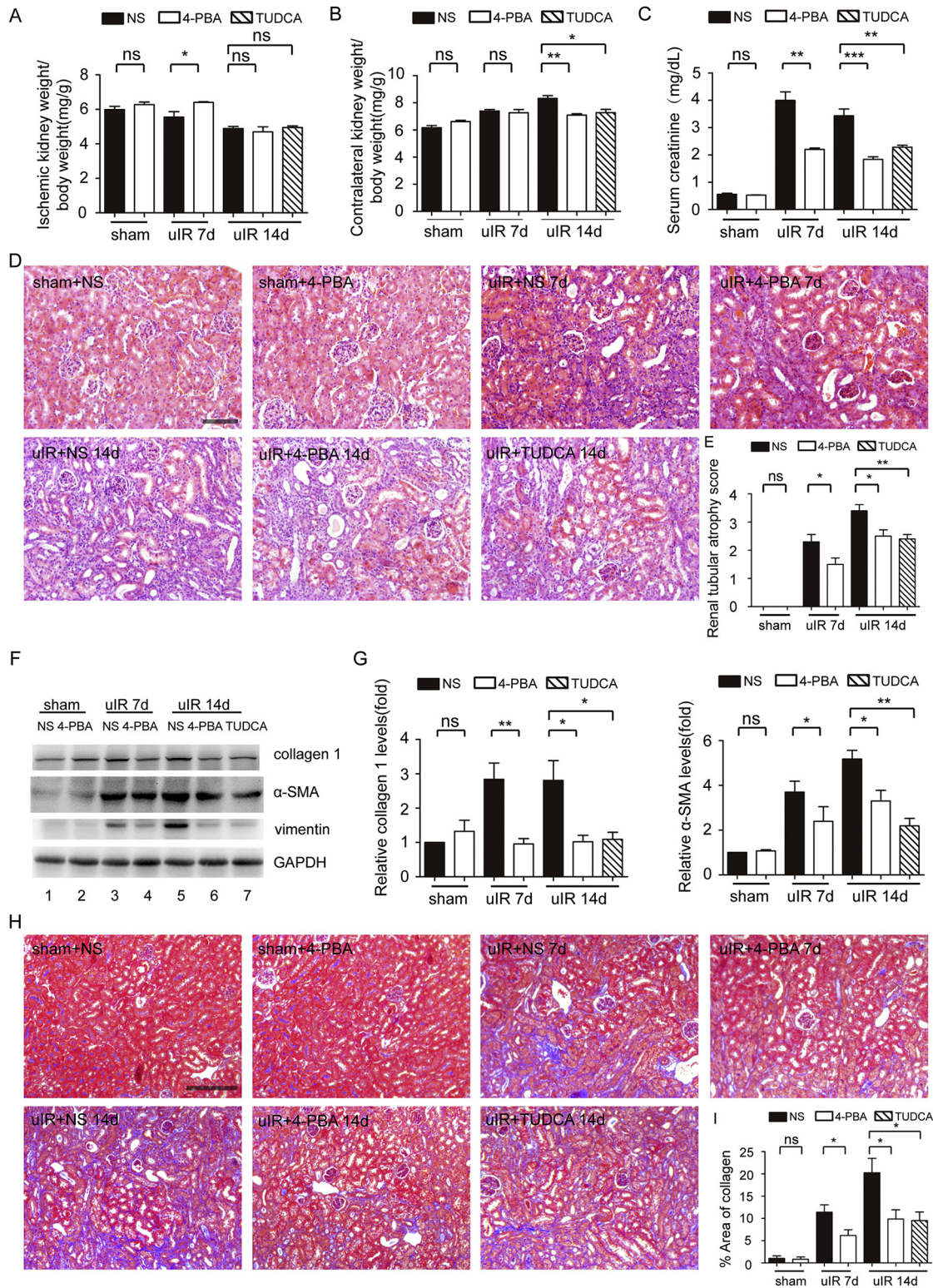


Fig. 4. 4-PBA and TUDCA given after IRI attenuates renal tubular atrophy, renal dysfunction and renal fibrosis. C57BL/6 mice (male, 8–10 week old) were subjected to 30 min of unilateral ischemia followed by reperfusion. 4-PBA at 20 mg/kg/day, TUDCA at 250 mg/kg/day, or normal saline (NS) was given from day 3 after uIR. For biochemical and histological analyses, kidney tissues were collected at day 7 or day 14. To determine the function of post-ischemic left kidney, right nephrectomy was performed one day before animal sacrifice and blood samples were then collected at animal sacrifice to measure serum creatinine. (A) Ischemic kidney weight/body weight (mg/g). (B) Contralateral kidney weight/body weight (mg/g). (C) Serum creatinine (mg/dL). (D) Representative renal images of hematoxylin-eosin staining. Bar = 200 μ m. (E) Pathological score of tubular atrophy. (F) Representative immunoblots of collagen 1, α -SMA, vimentin and GAPDH. GAPDH was used as a loading control. (G) Quantitative analysis of immunoblot of collagen 1 and α -SMA. For densitometric analysis, the protein level of sham group was arbitrarily set as 1, and the signals of other conditions were normalized with the sham control group to indicate their protein fold changes. (H) Representative images of Masson trichrome staining. Bar = 200 μ m. (I) Quantitative analysis of Masson trichrome staining. Data are expressed as mean \pm SEM. n = 4. *p < 0.05; **p < 0.01; ***p < 0.001; ns, not significant.

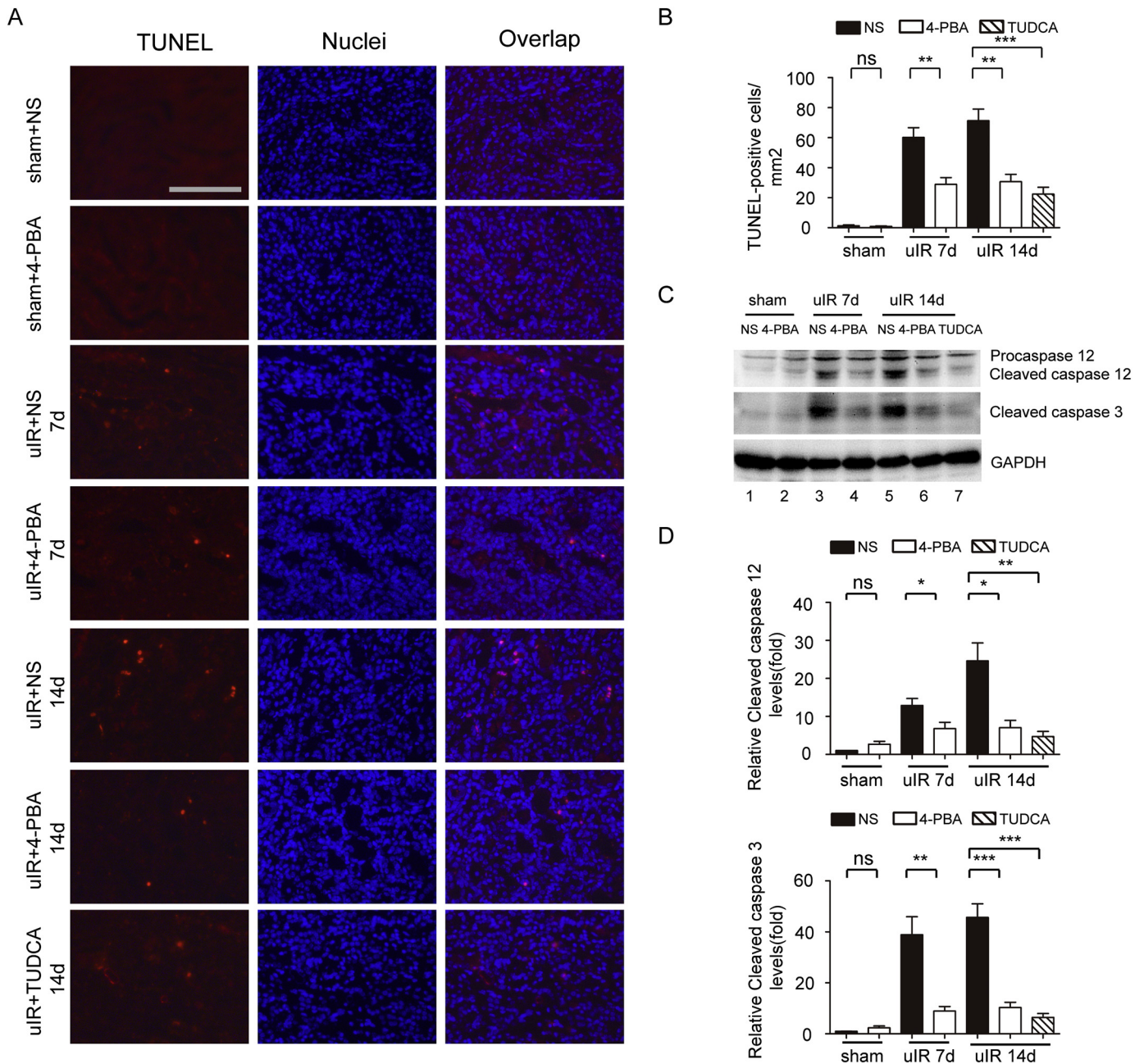


Fig. 5. 4-PBA and TUDCA given after IRI alleviates renal tubular cell apoptosis. C57Bl/6 mice were subjected to 30 min of left uIR or sham-operation. 4-PBA at 20 mg/kg/day, TUDCA at 250 mg/kg/day, or normal saline (NS) was given from day 3 after uIR. Kidney tissues were collected for biochemical and histological analyses. (A) Representative images of TUNEL staining. Bar = 200 μ m. (B) Quantitative analysis of TUNEL staining positive cells. (C) Representative immunoblots of cleaved caspase 12, cleaved caspase 3, and GAPDH (loading control). (D) Quantitative analysis of immunoblots of cleaved caspase 12 and cleaved caspase 3. For densitometric analysis, the protein level of sham group was arbitrarily set as 1, and the signals of other conditions were normalized with the sham control group to indicate their protein fold changes. Data are expressed as mean \pm SEM. n = 4. *p < 0.05; **p < 0.01; ***p < 0.001; ns, not significant.

Collective, these results suggest that ER stress promotes autophagy during AKI-CKD transition.

4. Discussion

ER stress has been implicated in the pathogenesis of AKI and CKD, but its involvement in the development of chronic renal pathologies after AKI, i.e. AKI-CKD transition, remains largely unknown. In the present study, we have demonstrated a sustained activation of ER stress in a mouse model of AKI-CKD transition induced by unilateral renal ischemia-reperfusion injury. Notably, pharmacological inhibition of ER stress after AKI markedly attenuated renal tubular atrophy and fibrosis, accompanied by better recovery of renal function in post-IRI kidneys.

Mechanistically, pharmacological inhibition of ER stress after AKI reduced tubular cell apoptosis, inflammation and autophagy, contributing to kidney repair and functional recovery.

Recent studies have suggested the involvement of ER stress in renal fibrosis [23,32,33]. In the present study, we have provided substantial evidence to support a role of ER stress in post-AKI fibrosis. We showed that ER stress was activated and sustained in renal proximal tubular cell after initial injury, as indicated by the induction of three well-known ER stress markers: p-PERK, BiP and CHOP. Moreover, inhibition of ER stress by 4-PBA and TUDCA 3 days after uIR significantly reduced post-AKI renal fibrosis and tubular atrophy, and partially restored renal functions. The timing of drug administration was critical in our study, because given after AKI would not affect initial kidney injury providing

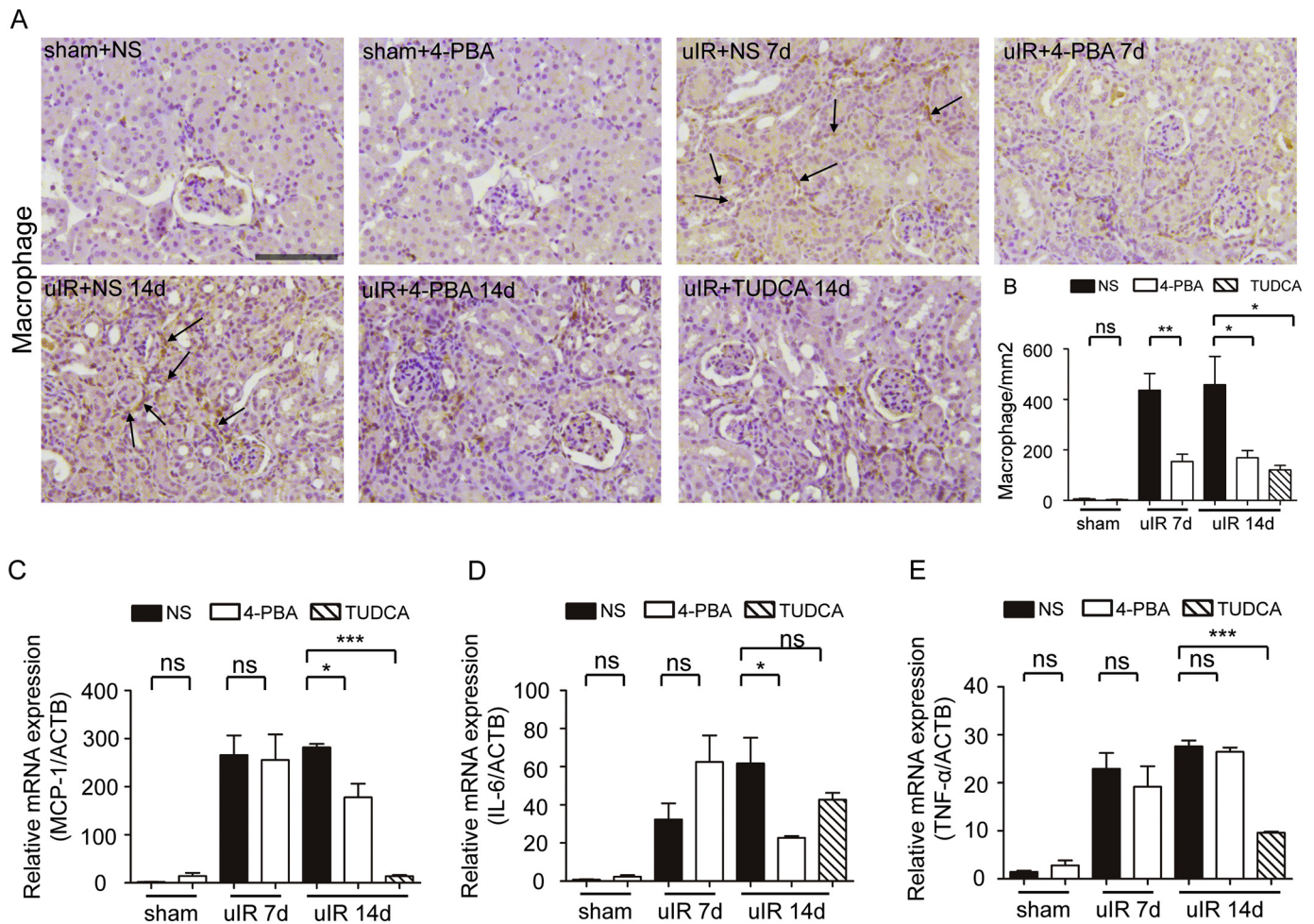


Fig. 6. 4-PBA and TUDCA given after IRI reduces renal interstitial inflammation. C57Bl/6 mice were subjected to 30 min of left uIR or sham-operation. 4-PBA at 20 mg/kg/day, TUDCA at 250 mg/kg/day, or normal saline (NS) was given from day 3 after uIR to collect kidney tissues for analyses. (A) Representative images of immunohistochemical staining of F4/80 to show macrophages. Arrows were used to indicate a few positive macrophages. Bar = 200 μ m. (B) Quantitative analysis of macrophages. (C–E) Real-time PCR analysis of MCP-1, IL-6, TNF- α and ACTB (internal control). Data are expressed as mean \pm SEM. $n = 4$. * $p < 0.05$; ** $p < 0.01$; *** $p < 0.001$; ns, not significant.

a condition to investigate the specific effect on kidney repair. Otherwise, if provided before or during AKI, 4-PBA and TUDCA may affect the severity of AKI making it difficult to determine the specific effect on AKI-CKD transition [18].

Of note, in addition to the function as an ER stress inhibitor [26], 4-PBA may also act as a weak histone deacetylase inhibitor (HDACi) [34]. HDACis have kidney protective effects in both AKI and CKD models [35–38]. Nonetheless, inhibition of histone acetylation by 4-PBA requires much higher doses (100 mg/kg/day) than that (20 mg/kg/day) for ER stress [39]. Our current study used 20 mg/kg/day 4-PBA that suppressed ER stress without changing histone acetylation according to previous work [39]. Moreover, TUDCA, another chemical chaperone tested in our study, had similar anti-fibrosis effects as 4-PBA in post-IRI kidneys. Together, these findings support a critical role of ER stress in the development of chronic pathologies, especially renal fibrosis, during AKI-CKD transition.

It is entirely unclear how ER stress promotes the development of chronic renal pathologies in post-AKI kidney. Recent studies have shown that, after severe or episodic AKI, renal tubular epithelial cells undergo a dramatic phenotypic change, leading to tubular cell death and atrophy as well as persistent production and secretion of profibrotic factors [8–11]. The phenotypic change may involve complex mechanisms, such as renal tubular cell cycle arrest [40], mitochondrial damage [41], autophagy [42] and senescence [43]. In the present study, we specifically examined the effects of ER stress

inhibitors on renal tubular cell apoptosis, autophagy, and inflammation in post-IRI kidneys.

In our study, ER stress inhibitors attenuated tubular cell apoptosis in post-IRI kidneys (Fig. 5). Interestingly, these inhibitors also prevented the activation of caspase-12, as indicated by caspase-12 cleavage. Caspase-12 is localized in the ER and plays an important role in ER stress-associated apoptosis. Activated caspase-12 can cleave caspase-9, which in turn cleaves procaspase-3 for its activation leading to apoptosis [44]. Thus, our current results support the activation and role of ER stress pathway of apoptosis in tubular cell death during AKI-CKD transition. Nonetheless, it is important to point out that the effects of ER stress inhibitors are significant but partial (Fig. 5), suggesting the involvement of other apoptotic pathways. In our study, BiP was induced at 2 days after IRI whereas CHOP was dramatically induced only at 14 days (Fig. 2). The time-dependent induction of these two ER stress proteins may be related to tubular cell death, because BiP may be an early adaptive or protective response whereas CHOP is known to have a pro-apoptotic function. Consistently, we detected the shuttling of CHOP to the nucleus after 7–14 days after IRI (Fig. 2E), which is an indication of transcriptional activation of CHOP for the induction of proapoptotic factors [9–11].

Inflammation is a common pathological feature of AKI [45]. After AKI, the intensity of inflammation may decrease but it may become chronic and contribute to AKI-CKD transition. Indeed, inflammation is known to be an important factor for renal fibrogenesis [46,47]. In our

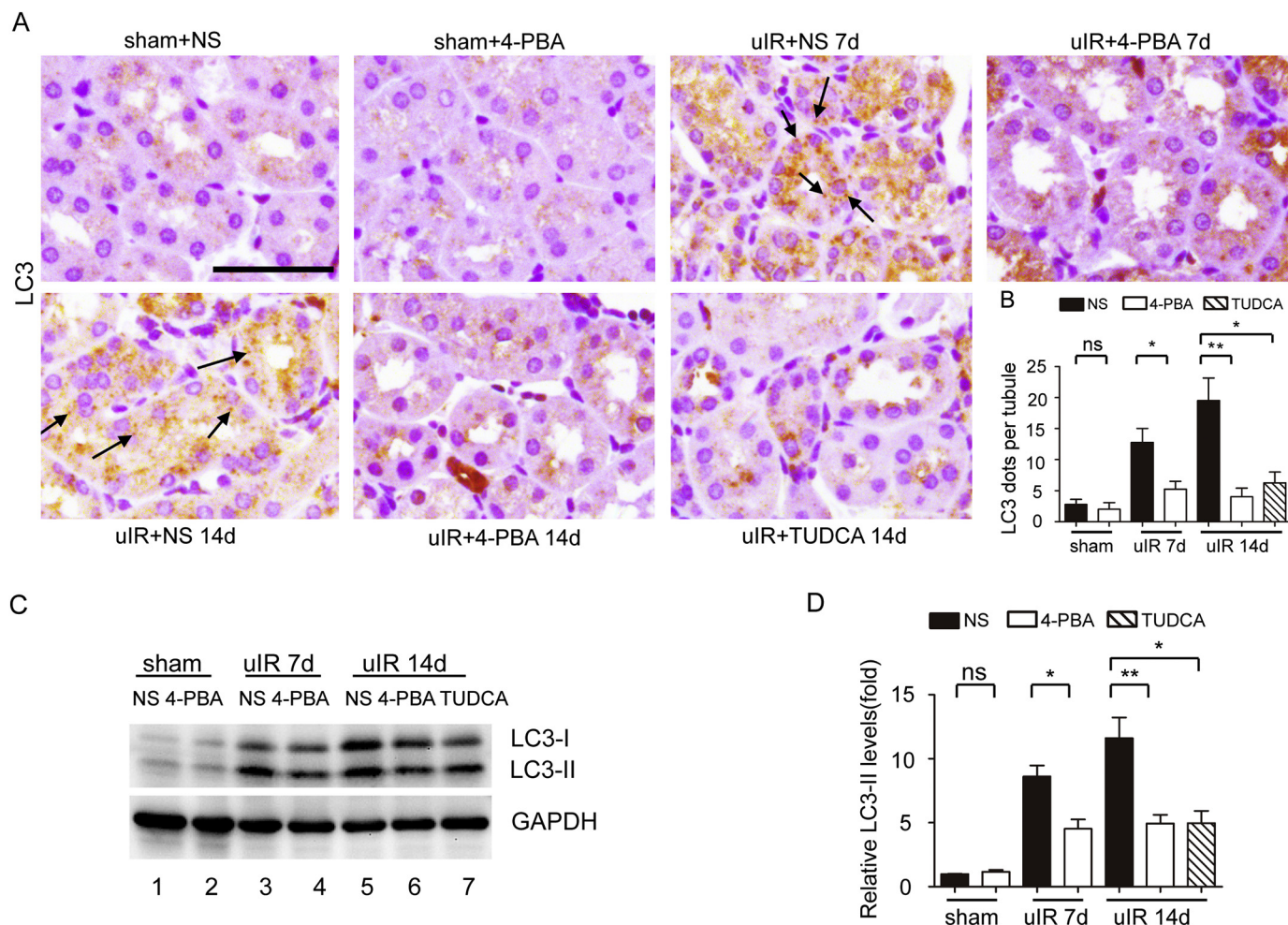


Fig. 7. 4-PBA and TUDCA given after IRI reduces renal tubular autophagy. Mice were subjected to 30 min of left uIR or sham-operation. 4-PBA at 20 mg/kg/day, TUDCA at 250 mg/kg/day, or normal saline (NS) was given from day 3 after uIR to collect kidney tissues for analyses. (A) Representative images of immunohistochemical staining of LC3. Arrows were used to indicate a few positive LC3 puncta or dots. Bar = 200 μ m. (B) Quantitative analysis of LC3 dots. (C) Representative immunoblot images of LC3B and GAPDH. GAPDH was used as a loading control. (D) Quantitative analysis of immunoblot of LC3B-II. For densitometric analysis, the protein level of sham group was arbitrarily set as 1, and the signals of other conditions were normalized with the sham control group to indicate their protein fold changes. Data are expressed as mean \pm SEM. n = 4 mice. *p < 0.05; **p < 0.01; ***p < 0.001; ns, not significant.

study, post-IRI kidneys showed macrophage infiltration, which was suppressed by both 4-PBA and TUDCA (Fig. 6). In addition, post-IRI kidneys showed the induction of pro-inflammatory cytokines, such as MCP-1, IL-6, and TNF- α . Interestingly, while 4-PBA and TUDCA generally suppressed the expression of pro-inflammatory cytokines, their effects towards specific cytokines were different. For example, 4-PBA was more effective in suppressing IL-6 at day 14 post-IRI, whereas TUDCA appeared more effective towards MCP-1 and TNF- α . Thus, these two chemical chaperones may have preference in targeting different immune cells.

By analyzing autophagosome numbers and LC3-II accumulation, we showed the evidence of persistent autophagy in renal tubule cells during AKI-CKD transition (Fig. 7). Both 4-PBA and TUDCA suppressed tubular autophagy when given after initial acute injury, suggesting the involvement of ER stress in autophagy under this condition. Autophagy is a cellular process of “self-eating”. In the present study, tubular autophagy apparently may account to tubular atrophy, which is the depletion of cytoplasm. In addition, tubular autophagy has been demonstrated to contribute to renal interstitial fibrosis [27,48], despite some controversies [49,50]. In the present study, 4-PBA and TUDCA suppressed tubular autophagy as well as renal fibrosis, supporting a pro-fibrosis role of autophagy in post-AKI kidneys.

There are several limitations in our study. For example, we only used pharmacological inhibitors without tissue or cell type specific genetic inhibitory approaches. The inhibitory effect was therefore systemic and not specific to renal tubules. In addition, our study tested the effects in the model of kidney repair following renal uIR. But clinically, there are multiple causes of kidney injury and post-injury renal fibrosis. Further studies need to determine the involvement of ER stress in kidney repair after nephrotoxic and sepsis-associated AKI.

In conclusion, we have demonstrated the sustained activation of ER stress in proximal tubules after AKI. ER stress may contribute to the development of chronic renal pathologies by promoting tubular atrophy, tubular cell death and interstitial inflammation. Thus, inhibition of ER stress may be a useful therapeutic strategy for the prevention of AKI-CKD transition following initial kidney injury.

Funding sources

The work was supported partly by the grants from National Natural Science Foundation of China (81720108008, 81430017), the National Institutes of Health of USA, and Department of Veterans Administration of USA.

The funding agencies had no role in study design, data collection, data analysis, interpretation, or writing of the report.

Supplementary data to this article can be found online at <https://doi.org/10.1016/j.ebiom.2018.10.006>.

Acknowledgements

We thank Dr. Man J. Livingston at Augusta University (Augusta, USA) for providing technical advice for some of the experiments in this study. We also thank all laboratory members of the Department of Nephrology and the Animal Facility staff at the Second Xiangya Hospital (Changsha, China) for their support.

Conflict of interests

The authors had no conflict of interests to declare.

Authors' contributions

Z.D., C.T., and S.S. conceived the idea and designed the study. S.S., J.Z., and Z.L. conducted most of the experiments. All authors contributed to data analysis and the preparation, writing and final approval of the manuscript.

References

- Mehta RL, Kellum JA, Shah SV, Molitoris BA, Ronco C, Warnock DG, et al. Acute kidney injury network: Report of an initiative to improve outcomes in acute kidney injury. *Crit Care* 2007;11(2):R31.
- Chawla LS, Eggers PW, Star RA, Kimmel PL. Acute kidney injury and chronic kidney disease as interconnected syndromes. *N Engl J Med* 2014;371(1):58–66.
- He L, Wei Q, Liu J, Yi M, Liu Y, Liu H, et al. AKI on CKD: Heightened injury, suppressed repair, and the underlying mechanisms. *Kidney Int* 2017;92(5):1071–83.
- Venkatachalam MA, Weinberg JM, Kriz W, Bidani AK. Failed tubule recovery, AKI-CKD transition, and kidney disease progression. *J Am Soc Nephrol* 2015;26(8):1765–76.
- Agarwal A, Dong Z, Harris R, Murray P, Parikh SM, Rosner MH, et al. Cellular and molecular mechanisms of AKI. *J Am Soc Nephrol* 2016;27(5):1288–99.
- Havasi A, Borkan SC. Apoptosis and acute kidney injury. *Kidney Int* 2011;80(1):29–40.
- Linkermann A, Chen G, Dong G, Kunzendorf U, Krautwald S, Dong Z. Regulated cell death in AKI. *J Am Soc Nephrol* 2014;25(12):2689–701.
- Humphreys BD. Mechanisms of renal fibrosis. *Annu Rev Physiol* 2018;80:309–26.
- Grgic I, Campanholle G, Bijol V, Wang C, Sabbisetti VS, Ichimura T, et al. Targeted proximal tubule injury triggers interstitial fibrosis and glomerulosclerosis. *Kidney Int* 2012;82(2):172–83.
- Humphreys BD, Cantaluppi V, Portilla D, Singbartl K, Yang L, Rosner MH, et al. Targeting endogenous repair pathways after AKI. *J Am Soc Nephrol* 2016;27(4):990–8.
- Basile DP, Bonventre JV, Mehta R, Nangaku M, Unwin R, Rosner MH, et al. Progression after AKI: Understanding maladaptive repair processes to predict and identify therapeutic treatments. *J Am Soc Nephrol* 2016;27(3):687–97.
- Yin J, Wang F, Yi Kong, R1 Wu, G4 Zhang, Wang N, et al. Antithrombin III prevents progression of chronic kidney disease following experimental ischaemic-reperfusion injury. *J Cell Mol Med* 2017;21(12):3506–14.
- Inagi R, Ishimoto Y, Nangaku M. Proteostasis in endoplasmic reticulum—new mechanisms in kidney disease. *Nat Rev Nephrol* 2014;10(7):369–78.
- Cybulsky AV. Endoplasmic reticulum stress, the unfolded protein response and autophagy in kidney diseases. *Nat Rev Nephrol* 2017;13(11):681–96.
- Yan M, Shu S, Guo C, Tang C, Dong Z. Endoplasmic reticulum stress in ischemic and nephrotoxic acute kidney injury. *Ann Med* 2018;1–24.
- Gao X, Fu L, Xiao M, Xu C, Sun L, Zhang T, et al. The nephroprotective effect of tauroursodeoxycholic acid on ischaemia/reperfusion-induced acute kidney injury by inhibiting endoplasmic reticulum stress. *Basic Clin Pharmacol Toxicol* 2012;111(1):14–23.
- Xu Y, Guo M, Jiang W, Dong H, Han Y, An XF, et al. Endoplasmic reticulum stress and its effects on renal tubular cells apoptosis in ischemic acute kidney injury. *Ren Fail* 2016;38(5):831–7.
- Inagi R, Nangaku M, Onogi H, Ueyama H, Kitao Y, Nakazato K, et al. Involvement of endoplasmic reticulum (ER) stress in podocyte injury induced by excessive protein accumulation. *Kidney Int* 2005;68(6):2639–50.
- Wu J, Zhang R, Torreggiani M, Ting A, Xiong H, Striker GE, et al. Induction of diabetes in aged C57B6 mice results in severe nephropathy: An association with oxidative stress, endoplasmic reticulum stress, and inflammation. *Am J Pathol* 2010;176(5):2163–76.
- Chiang CK, Hsu SP, Wu CT, Huang JW, Cheng HT, Chang YW, et al. Endoplasmic reticulum stress implicated in the development of renal fibrosis. *Mol Med* 2011;17(11–12):1295–305.
- Liu SH, Yang CC, Chan DC, Wu CT, Chen LP, Huang JW, et al. Chemical chaperon 4-phenylbutyrate protects against the endoplasmic reticulum stress-mediated renal fibrosis in vivo and in vitro. *Oncotarget* 2016;7(16):22116–27.
- Xiao W, Fan Y, Wang N, Chuang PY, Lee K, He JC. Knockdown of RTN1A attenuates ER stress and kidney injury in albumin overload-induced nephropathy. *Am J Physiol Renal Physiol* 2016;310(5):F409–15.
- Fan Y, Xiao W, Lee K, Salem F, Wen J, He L, et al. Inhibition of reticulon-1A-mediated endoplasmic reticulum stress in early AKI attenuates renal fibrosis development. *J Am Soc Nephrol* 2017.
- Fu Y, Tang C, Cai J, Chen G, Zhang D, Dong Z. Rodent models of AKI-CKD transition. *Am J Physiol Renal Physiol* 2018 Jun 27. <https://doi.org/10.1152/ajprenal.00199.2018> (Epub ahead of print).
- Skrypnik NI, Harris RC, de Caestecker MP. Ischemia-reperfusion model of acute kidney injury and post injury fibrosis in mice. *J Vis Exp* 2013 Aug 9(78). <https://doi.org/10.3791/50495>.
- Cao AL, Wang L, Chen X, Wang YM, Guo HJ, Chu S, et al. Ursodeoxycholic acid and 4-phenylbutyrate prevent endoplasmic reticulum stress-induced podocyte apoptosis in diabetic nephropathy. *Lab Invest* 2016;96(6):610–22.
- Livingston MJ, Ding HF, Huang S, Hill JA, Yin XM, Dong Z. Persistent activation of autophagy in kidney tubular cells promotes renal interstitial fibrosis during unilateral ureteral obstruction. *Autophagy* 2016;12(6):976–98.
- Ding WX, Yin XM. Sorting, recognition and activation of the misfolded protein degradation pathways through macroautophagy and the proteasome. *Autophagy* 2008;4(2):141–50.
- Gao Y, Zhu H, Yang F, Wang Q, Feng Y, Zhang C. Glucocorticoid-activated IRE1alpha/XBP-1s signaling: An autophagy-associated protective pathway against endothelial cell damage. *Am J Physiol Cell Physiol* 2018;315(3):C300–9.
- Kawakami T, Inagi R, Takano H, Sato S, Ingelfinger JR, Fujita T, et al. Endoplasmic reticulum stress induces autophagy in renal proximal tubular cells. *Nephrol Dial Transplant* 2009;24(9):2665–72.
- Li W, Yang Q, Mao Z. Signaling and induction of chaperone-mediated autophagy by the endoplasmic reticulum under stress conditions. *Autophagy* 2018;1–3.
- Liu Y, Wang Y, Ding W. Mito-TEMPO alleviates renal fibrosis by reducing inflammation, mitochondrial dysfunction, and endoplasmic reticulum stress. *2018*; 5828120.
- Kim H, Baek CH, Lee RB, Chang JW, Yang WS, Lee SK. Anti-fibrotic effect of losartan, an angiotensin II receptor blocker, is mediated through inhibition of ER stress via Up-regulation of SIRT1, followed by induction of HO-1 and thioredoxin. *Int J Mol Sci* 2017;18(2).
- Miller AC, Cohen S, Stewart M, Rivas R, Lison P. Radioprotection by the histone deacetylase inhibitor phenylbutyrate. *Radiat Environ Biophys* 2011;50(4):585–96.
- Levine MH, Wang Z, Bhatti TR, Wang Y, Aufhauser DD, McNeal S, et al. Class-specific histone/protein deacetylase inhibition protects against renal ischemia reperfusion injury and fibrosis formation. *Am J Transplant* 2015;15(4):965–73.
- Cianciolo Cosentino C, Skrypnik NI, Brilli LL, Chiba T, Novitskaya T, Woods C, et al. Histone deacetylase inhibitor enhances recovery after AKI. *J Am Soc Nephrol* 2013;24(6):943–53.
- Liu J, Livingston MJ, Dong G, Tang C, Su Y, Wu G, et al. Histone deacetylase inhibitors protect against cisplatin-induced acute kidney injury by activating autophagy in proximal tubular cells. *Cell Death Dis* 2018;9(3):322.
- Pang M, Kothapally J, Mao H, Tolbert E, Ponnusamy M, Chin YE, et al. Inhibition of histone deacetylase activity attenuates renal fibrotic activation and interstitial fibrosis in obstructive nephropathy. *Am J Physiol Renal Physiol* 2009;297(4):F996–F1005.
- Luo T, Chen B, Wang X. 4-PBA prevents pressure overload-induced myocardial hypertrophy and interstitial fibrosis by attenuating endoplasmic reticulum stress. *Chem Biol Interact* 2015;242:99–106.
- Yang L, Besschetnova TY, Brooks CR, Shah JV, Bonventre JV. Epithelial cell cycle arrest in G2/M mediates kidney fibrosis after injury. *Nat Med* 2010;16(5):535–43 (531p following 143).
- Tang C, Han H, Yan M, Zhu S, Liu J, Liu Z, et al. PINK1-PRKN/PARK2 pathway of mitophagy is activated to protect against Renal ischemia-reperfusion injury. *Autophagy* 2018;1–18.
- He L, Livingston MJ, Dong Z. Autophagy in acute kidney injury and repair. *Nephron Clin Pract* 2014;127(1–4):56–60.
- Luo C, Zhou S, Zhou Z, Liu Y, Yang L, Liu J, et al. Wnt9a promotes renal fibrosis by accelerating cellular senescence in tubular epithelial cells. *2018*; 1238–56.
- Morishima N, Nakanishi K, Takenouchi H, Shibata T, Yasuhiko Y. An endoplasmic reticulum stress-specific caspase cascade in apoptosis. Cytochrome c-independent activation of caspase-9 by caspase-12. *J Biol Chem* 2002;277(37):34287–94.
- Jang HR, Rabb H. Immune cells in experimental acute kidney injury. *Nat Rev Nephrol* 2015;11(2):88–101.
- Liu Y. Cellular and molecular mechanisms of renal fibrosis. *Nat Rev Nephrol* 2011;7(12):684–96.
- Rabb H, Griffin MD, McKay DB, Swaminathan S, Pickers P, Rosner MH, et al. Inflammation in AKI: Current understanding, key questions, and knowledge gaps. *J Am Soc Nephrol* 2016;27(2):371–9.
- Baisanry A, Bhayana S, Rong S, Ermeling E, Wrede C, Hegermann J, et al. Autophagy induces prosenescence changes in proximal tubular S3 segments. *J Am Soc Nephrol* 2016;27(6):1609–16.
- Ding Y, Kim S, Lee SY, Koo JK, Wang Z, Choi ME. Autophagy regulates TGF-beta expression and suppresses kidney fibrosis induced by unilateral ureteral obstruction. *J Am Soc Nephrol* 2014;25(12):2835–46.
- Li H, Peng X, Wang Y, Cao S, Xiong L, Fan J, et al. Atg5-mediated autophagy deficiency in proximal tubules promotes cell cycle G2/M arrest and renal fibrosis. *Autophagy* 2016;1–15.
- Jiang M, Wei Q, Dong G, Komatsu M, Su Y, Dong Z. Autophagy in proximal tubules protects against acute kidney injury. *Kidney Int* 2012;82(12):1271–83.